

NANO EXPRESS

Open Access

Quantum dot-doped porous silicon metal–semiconductor metal photodetector

Chia-Man Chou¹, Hsing-Tzu Cho², Vincent K S Hsiao^{2*}, Ken-Tye Yong³ and Wing-Cheung Law⁴

Abstract

In this paper, we report on the enhancement of spectral photoresponsivity of porous silicon metal–semiconductor metal (PS-MSM) photodetector embedded with colloidal quantum dots (QDs) inside the pore layer. The detection efficiency of QDs/PS hybrid-MSM photodetector was enhanced by five times larger than that of the undoped PS-MSM photodetector. The bandgap alignment between PS (approximately 1.77 eV) and QDs (approximately 1.91 eV) facilitates the photoinduced electron transfer from QDs to PS whereby enhancing the photoresponsivity. We also showed that the photoresponsitivity of QD/PS hybrid-MSM photodetector depends on the number of layer coatings of QDs and the pore sizes of PS.

Keywords: Porous silicon, Quantum dots, Photodetector

Background

Colloidal quantum dots (QDs) are semiconductor nanocrystals with tunable optical property depending on their sizes and shapes that can be controlled by the fabrication process. Outstanding optoelectronic and photonic properties, such as electroluminescence, photoluminescence, photovoltaics, absorption, and narrow emission linewidth, make QDs a good candidate for photodetectors [1-6], light emitting diodes [7-9] and lasers applications [10-12]. Because of the QDs' inherent solution-processable property, several studies have incorporated QDs into organic or inorganic matrix and demonstrated these hybrid devices with improved optoelectronic performances [13-20]. In this paper, we report on the enhancement of photoresponsivity in inorganic/inorganic hybrid device consisting of porous silicon (PS)-MSM (metal–semiconductor–metal) photodetector and CdSe/CdS/ZnS core shell QDs embedded in the pores within the PS. The bandgap alignment between PS (approximately 1.77 eV) and QDs (approximately 1.91 eV) facilitates the photoinduced electron transfer from QDs to PS and further enhances the photoresponsivity. We also show that the photoresponsitivity depends on the numbers of coating of

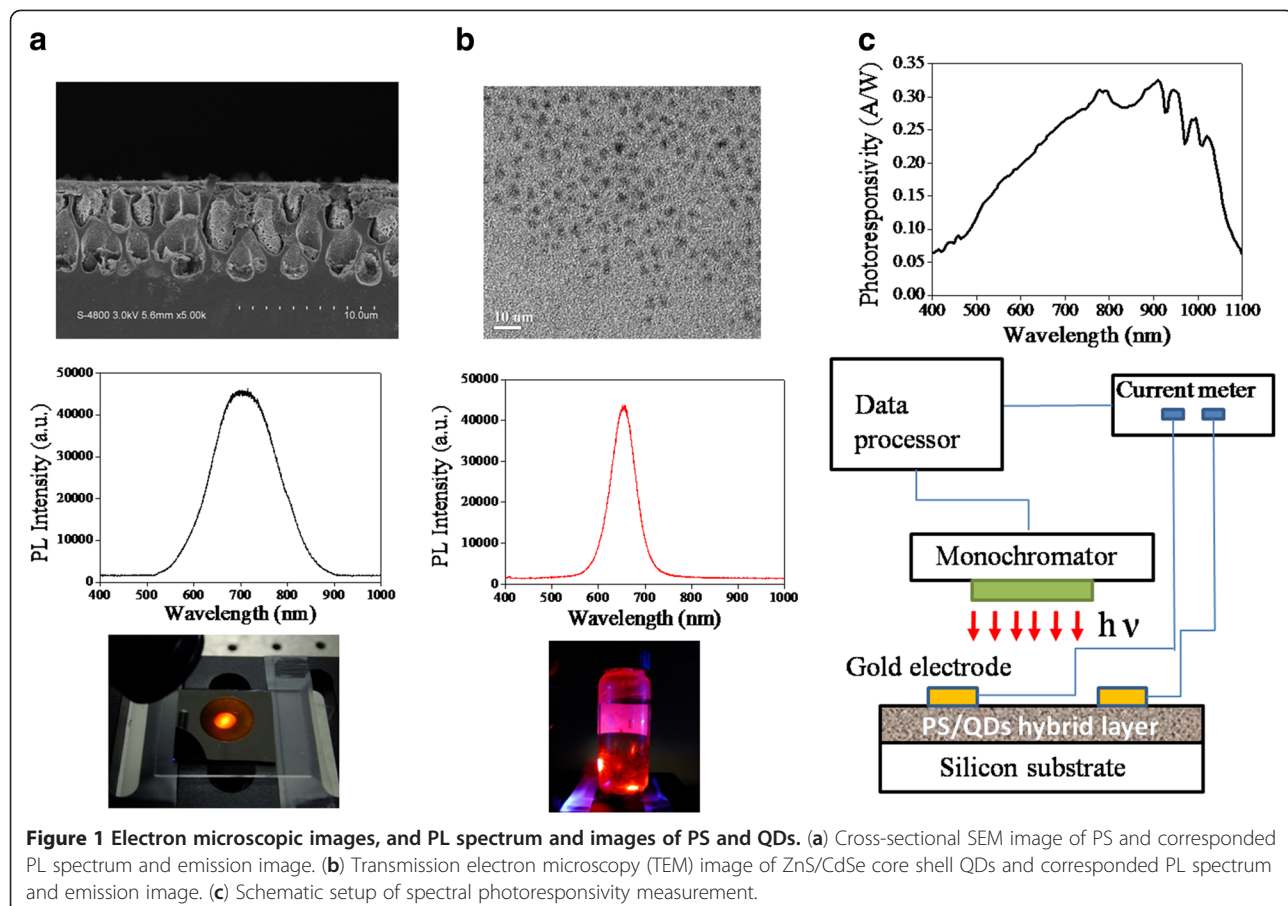
QDs and the pore size of PS which could be controlled by the anodization time.

Methods

The PS layers were fabricated by anodic etching where a p-type silicon substrate was placed in the homemade Teflon (E.I. du Pont de Nemours and Company, Wilmington, DE, USA) etching cell using a mixture of aqueous hydrogen fluoride (purity 49%) and ethanol (purity 99%), 1:1 by volume. The sample was anodized at current density of 16 mA/cm² and at different time. No further chemical or thermal treatment was carried after etching. A stainless steel shadow mask with the MSM finger pattern of spacing and width of about 100 and 100 μm, respectively, was fabricated by micromachining process. The MSM finger pattern was formed by Au metal thermal evaporation. The CdSe/CdS/ZnS core-shell colloidal QDs absorbed on the internal pores within PS were then prepared by dipping the PS using CdSe/CdS/ZnS QDs (0.6 mg) dissolved in toluene (100 mg) and evaporating toluene at room temperature for 30 min. Figure 1a shows the cross-sectional image of anodized PS captured by scanning electronic microscopy (SEM). The average pore depth is about 8 μm. Figure 1a, middle image, also show the photoluminescence (PL) spectrum and fluorescence emission images of PS, indicating a PL emission wavelength of approximately 700 nm (approximately 1.77 eV). The CdSe/CdS/ZnS

* Correspondence: kshsiao@ncnu.edu.tw

²Department of Applied Materials and Optoelectronic Engineering, National Chi Nan University, No. 1, University Rd, Puli, NanTou 54561, Taiwan
Full list of author information is available at the end of the article



core-shell colloidal QDs were prepared by growing a CdS/ZnS shell on a CdSe core [21]. For core CdSe QDs, they can be synthesized at 300°C by the reaction between cadmium oxide dissolved in oleic acid and trioctylphosphine (TOP) and TOPSe. The reaction resulted in the formation of monodispersed CdSe QDs. The shell growth of CdS and ZnS was uniform and epitaxial and eventually coats onto the CdSe core. The average diameter of core shell QDs was approximately 5 nm, as shown in Figure 1b. Figure 1b also shows the PL spectrum and image of fluorescence emission of QDs, indicating a PL emission wavelength of approximately 650 nm (approximately 1.99 eV). Photoresponsivity measurements were performed at room temperature employing a light source (50 W halogen lamp) equipped with a monochromator (Acton SP2155, Princeton Instruments Inc., Trenton, NJ, USA) and a current meter (Keithley 6485, Keithley Instruments Inc., Cleveland, OH, USA), as shown in Figure 1c. Figure 1c also shows the spectral photoresponstivity of standard silicon-based photodetector (SI 1337). The spectral photoresponstivity of fabricated MSM photodetector was determined relatively to the value measured from the standard silicon-based photodetector.

Results and discussion

Figure 2 (inset) shows the dark current of a PS-MSM photodetector before, curve (i), and after, curve (ii), doping QDs characterized by the *I-V* measurement. The

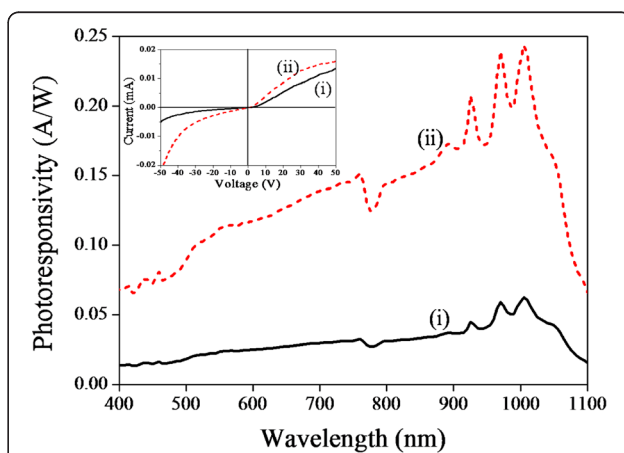


Figure 2 Comparison of spectral photoresponsivity and *I-V* curve from QD-doped and undoped samples. Comparison of spectral photoresponsivity and *I-V* curve (inset) from undoped (curve i) and QDs doped (curve ii) PS-MSM photodetector. The anodization time was 25 min. *I-V* curve was measured at dark environment.

increase of dark current indicates that the doped QDs enhance the charge transfer between PS and electrode. We speculate that the QDs may provide a shunt conduction path next to the PS that might explain the increase of the dark current. As expected from the symmetry of the MSM structure, the *I-V* characteristics in our current device should be symmetric; however, the *I-V* curve measured here are not perfect symmetry around zero. The discrepancy may be due to the inhomogeneous etching within the area ($10 \times 10 \text{ mm}^2$) of MSM device. Figure 2 shows that the photoresponsivity increases in doped QDs/PS hybrid-MSM photodetector comparing to undoped PS-MSM photodetector. Figure 3 proposes a model for electron transfer at the PS/QD interface in a QDs/PS hybrid-MSM photodetector sample. The bulk Si has indirect bandgap, but porous PS has direct bandgap. The energy-band structure of PS could be predicted by PL measurement of PS samples [22]. The direct bandgap semiconductors offer much stronger absorption coefficient; therefore, the PS has better optoelectronic properties than bulk Si. After adding QDs onto the PS sample, the band alignment between the two materials allows photoinduced electron transfer from the QDs to the PS. In addition, QD nanostructures could provide large surface areas and short diffusion lengths for photogenerated charge carriers [23]. The photoresponsivity behavior of QDs/PS hybrid-MSM photodetector was recorded by comparing to the photoresponsivity of the standard silicon-based photodetector, as shown in the inset from Figure 1c, so the enhancement of photoresponsivity from QDs/PS hybrid-MSM photodetector has maximum photoresponsivity at approximately 900 nm.

The anodization time of PS is an important parameter for the PS-MSM photodetector. Figure 4 shows spectral photoresponsivity of QDs/PS hybrid-MSM photodetector for various anodization times. The anodization current density was 20 mA/cm^2 . It is obvious that the photoresponsivity increases with increasing the anodization time. Figure 4 (inset) shows the PL spectrum dependent on anodization time. We observed that the peak wavelength within PL spectrum shifts from 720 to 700 nm indicating the energy bandgap of PS changes

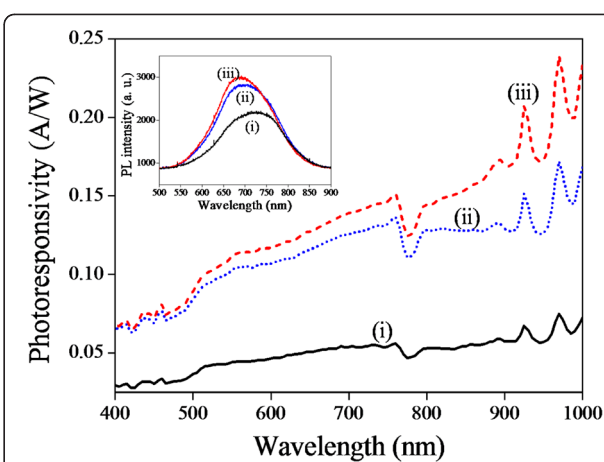
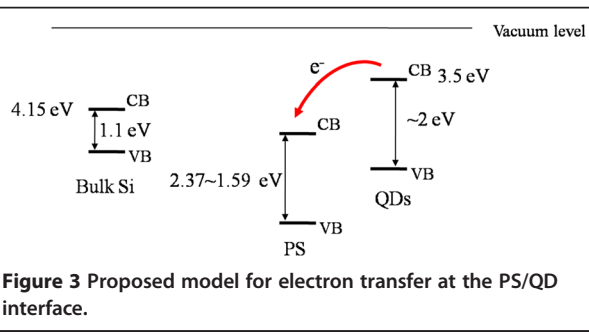


Figure 4 Comparison of spectral photoresponsivity and PL spectrum at different PS anodization times. Spectral photoresponsivity and PL spectrum (inset) of QDs/PS hybrid-MSM photodetector dependent on anodization times, 5 (i), 10 (ii) and 25 (iii) min, of porous silicon at 16 mA/cm^2 anodization current.

from 1.72 to 1.77 eV. Higher PS bandgap energy (1.77 eV) favors the bandgap alignment between PS and QDs (1.91 eV) and further enhances the photoresponsivity of QDs/PS hybrid-MSM photodetector.

Figure 5 shows the spectral photoresponsivity for the PS-MSM photodetector (control) and QDs/PS hybrid-MSM photodetector obtained after one, three, and five coatings. The photoresponsivity increases with increasing QD coating layers and reaches at maximum value when three coating layer processes was applied. However, we observed that the photoresponsivity decreases when five coatings process are applied on the PS-MSM photodetector. Figure 5 (inset) compares the optical microscopic images of the MSM device after different numbers of QD coating process. The yellow bright region is the

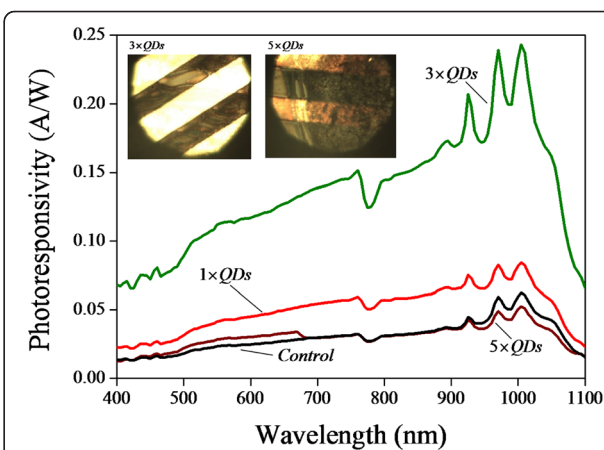


Figure 5 Spectral photoresponsivity dependent on the number of QD coatings. Spectral photoresponsivity and optical microscopic image (inset) of QDs/PS hybrid MSM photodetector dependent on the number of coatings. The anodization time was 25 min.

electrode while the dark brown region is the PS. We speculate that five-time coating processes make the QDs aggregate together and decrease the photoresponsivity.

Conclusions

We have presented an enhancement of the photoresponsivity of QDs/PS hybrid MSM photodetector. We found out that the bandgap alignment between QDs and PS facilitates the electron transfer and further increases the photoresponsivity. By choosing different anodization time and layers of QD coating, we demonstrate the flexibility in fabricating QDs/PS hybrid MSM photodetector.

Competing interests

The authors declare that they have no competing interests.

Authors' contributions

VKSH proposed the idea and helped in the preparation of the manuscript. CMC and HTC designed and carried out the experiment, analyzed the data, and prepared the manuscript. KTY and WCL carried out the fabrication of QDs and provided a helpful discussion. All authors read and approved the final manuscript.

Authors' information

VKSH received a Ph.D. from Electrical Engineering in SUNY at Buffalo in 2005. He is currently an associate professor in the Department of Applied Materials and Optoelectronic Engineering at National Chi Nan University, Taiwan. His research interests include organic/inorganic nanoporous materials, photoresponsive LC-based photonic devices, and optical thin films. CMC is a medical doctor at the Department of Surgery in Taichung Veterans General Hospital, Taiwan. HTC is an undergraduate student. KTY is an assistant professor at the Nanyang Technological University in the School of Electrical and Electronic Engineering. He received his Ph.D. from Chemical and Biological Engineering in SUNY at Buffalo in 2006. His research interests involve the synthesis, functionalization, and application of nanoparticles. WCL is a postdoctoral scholar in the Institute for Lasers, Photonics and Biophotonics (ILPB).

Acknowledgments

This study was supported by Taichung Veterans General Hospital/National Chi Nan University Joint Research Program (TCVGH-NCNU-1007903).

Author details

¹Division of Pediatric Surgery, Department of Surgery, Taichung Veterans General Hospital, 160 sec. 3 Chung-Kang Rd, Taichung 40705, Taiwan.

²Department of Applied Materials and Optoelectronic Engineering, National Chi Nan University, No. 1, University Rd, Puli, NanTou 54561, Taiwan. ³School of Electrical and Electronic Engineering, Nanyang Technological University, Nanyang 639798, Singapore. ⁴Institute for Lasers, Photonics, and Biophotonics, University at Buffalo, The State University of New York, Buffalo, NY 14260-4200, USA.

Received: 5 April 2012 Accepted: 23 May 2012

Published: 6 June 2012

References

- McDonald SA, Konstantatos G, Zhang S, Cyr PW, Klem EJD, Levina L, Sargent EH: Solution-processed PbS quantum dot infrared photodetectors and photovoltaics. *Nat Mater* 2005, **4**:138–142.
- Konstantatos G, Howard I, Fischer A, Hoogland S, Clifford J, Klem E, Levina L, Sargent EH: Ultrasensitive solution-cast quantum dot photodetectors. *Nature* 2006, **442**:180–183.
- Shieh J-M, Yu W-C, Huang J-Y, Wang C-K, Dai B-T, Jhan H-Y, Hsu C-W, Kuo H-C, Yang F-L, Pan C-L: Near-infrared silicon quantum dots metal-oxide-semiconductor field-effect transistor photodetector. *Appl Phys Lett* 2009, **94**:241108.
- Tu C-C, Tang L, Huang J, Voutsas A, Lin LY: Solution-processed photodetectors from colloidal silicon nano/micro particle composite. *Opt Express* 2010, **18**:21622–21627.
- Nayfeh OM, Rao S, Smith A, Therrien J, Nayfeh MH: Thin film silicon nanoparticle UV photodetector. *IEEE Photo. Tech. Lett.* 2004, **16**:1927–1929.
- Passmore BS, Jiang Wu, Kunets VP, Lytvyn PM, Salamo GJ, Manasreh MO: Room temperature near-infrared photoresponse based on interband transitions in In_{0.35}Ga_{0.65}As multiple quantum dot photodetectors. *Electron Device Letters* 2008, **29**:224–227.
- Dabbousi BO, Bawendi MG, Onitsuka O, Rubner MF: Electroluminescence from CdSe quantum-dot/polymer composites. *Appl Phys Lett* 1995, **66**:1316–1318.
- Hikmet RAM, Chin PTK, Talapin DV, Weller H: Polarized-light-emitting quantum-rod diodes. *Adv Mater* 2005, **17**:1436–1439.
- Jiang Wu, Wang ZM, Dorogan VG, Li S, Li Z, Mazur YI, Salamo GJ: Near infrared broadband emission of In_{0.35}Ga_{0.65}As quantum dots on high index GaAs surfaces. *Nanoscale* 2011, **3**:1485–1488.
- Reitzenstein S, Bazhenov A, Gorbunov A, Hofmann C, Munch S, Loffler A, Kamp M, Reithmaier JP, Kulakovskii VD, Forchel A: Lasing in high-Q quantum-dot micropillar cavities. *Appl Phys Lett* 2006, **89**:051107.
- Gao S, Zhang C, Liu Y, Su H, Wei L, Huang T, Dellas N, Shang S, Mohney SE, Wang J: Lasing from colloidal InP/ZnS quantum dots. *Opt Express* 2011, **19**:5528–5535.
- Shchekin OB, Deppe DG: 1.3 μm InAs quantum dot laser with To = 161K from 0 to 80°C. *Appl Phys Lett* 2002, **80**:3277.
- Hoyer P, Koenkamp R: Photoconduction in porous TiO₂ sensitized by PbS quantum dots. *Appl Phys Lett* 1995, **66**:349–351.
- Huynh WU, Dittmer JJ, Alivisatos AP: Hybrid nanorod-polymer solar cells. *Science* 2002, **295**:2425–2427.
- Alguno A, Usami N, Ujihara T, Fujiwara K, Sazaki G, Nakajima K: Enhanced quantum efficiency of solar cells with self-assembled Ge dots stocked in multilayer structure. *Appl Phys Lett* 2003, **83**:1258–1260.
- Choudhury KR, Sahoo Y, Prasad PN: Hybrid quantum-dot-polymer nanocomposites for infrared photorefractivity at an optical communication wavelength. *Adv Mater* 2005, **17**:2877–2881.
- Li X, Chon JWM, Evans RA, Gu M: Quantum-rod dispersed photopolymers for multi-dimensional photonic applications. *Opt Express* 2009, **17**:2954–2961.
- Shieh J-M, Huang J-Y, Yu W-C, Huang J-D, Wang Y-C, Chen C-W, Wang C-K, Huang W-H, Cho A-T, Kuo H-C, Dai B-T, Yang F-L, Pan C-L: Nonvolatile memory with switching interfacial polar structures of nano Si-in-mesoporous silica. *Appl Phys Lett* 2009, **95**:143501.
- Huang JY, Shieh JM, Kuo HC, Pan CL: Interfacial polar-bonding-induced multifunctionality of nano-silicon in mesoporous silica. *Adv Funct Mater* 2009, **19**:2089–2094.
- Qiao H, Guan B, Böcking T, Gal M, Gooding JJ, Reece PJ: Optical properties of II-VI colloidal quantum dot doped porous silicon microcavities. *Appl Phys Lett* 2010, **96**:161106.
- Qian J, Yong K-T, Roy I, Ohulchansky TY, Bergey EJ, Lee HH, Tramposch KM, He S, Maitra A, Prasad PN: Imaging pancreatic cancer using surface-functionalized quantum dots. *J Phys Chem B* 2007, **111**:6969–6972.
- Egeberg RC, Veje E, Ferreira Da Silva A, Pepe I, Santos Alves A: The energy-band structure of porous silicon studied with photoluminescence excitation and photoacoustic spectroscopy. *J. Porous Mater* 2000, **7**:173–176.
- Tang J, Sargent EH: Infrared Colloidal Quantum Dots for Photovoltaics: Fundamentals and Recent Progress. *Adv Mater* 2011, **23**:12–29.

doi:10.1186/1556-276X-7-291

Cite this article as: Chou et al.: Quantum dot-doped porous silicon metal-semiconductor metal photodetector. *Nanoscale Research Letters* 2012 **7**:291.